A Reconfigurable Reflectarray Antenna With an 8 μm-Thick Layer of Liquid Crystal

Weiquan Zhang, Yue Li, *Senior Member, IEEE*, and Zhijun Zhang, *Fellow, IEEE*

***Abstract*— This article demonstrates an electronically scanned reflectarray antenna based on liquid crystal (LC). The LC-based reflectarray element was designed as a periodically loading of parallel H-shaped polygons on two metal layers. To realize a tunable reflection phase and reduce the inhomogeneity effect of LC, an 8 μm-thick LC layer was designed as a varactor rather than a substrate. In simulations, the adjustable reflection-phase range of the proposed element was 180° in the frequency band 21–21.5 GHz. The design concept was verified on a reflectarray prototype containing 26 rows of the basic elements. In addition, a 32-channel control circuit was designed and fabricated for biasing. The measured results confirmed a tunable phase range of 150° at 23.8 GHz. The disagreements between the simulated and measured results are discussed, and a test process is proposed. As a proof of concept, the main beam was steered to 0°, −40°, and −60° in one plane. The result confirmed the high beam-steering capability of the proposed reflectarray with measured gains above 18 dB at 23.8 GHz. This work provides useful references for the design and measurement of LC-based reflectarray antennas.**

***Index Terms*— Beam scanning reflectarray, liquid crystal (LC), liquid crystal display (LCD) technology, response speed.**

I. Introduction

REFLECTARRAY antennas have gained considerable interest owing to their low cost, ease of construction, and ability to electronically reconfigure the beam [1]. Reflectarray antennas also enable beam scanning, so they are widely used in satellite communication, radar, and imaging applications. The phase shift function of each element is the key problem in reflectarray antennas. The beam can be reconfigured using control devices or tunable materials. Suitable control devices are varactor diodes [2], [3], p-i-n diodes [4], [5], and the microelectromechanical systems switch [6]–[8], which alter the physical structure or resonant frequencies of the elements. The parasitic effect of diodes is nonnegligible in frequency bands above 10 GHz. Alternatively, the reflection phase can be changed by employing tunable materials, such as barium strontium titanate [9], ferrite [10], and liquid crystal (LC) [11]–[13]. As a low-cost and easily integrated material, LC is suitable for microwave-range applications, especially at frequencies higher than the Ku-band [14], [15].

Applying a changing quasi-static electric field to an LC material with alterable permittivity value can realize a reconfigurable antenna. In [16]–[19], transmission lines with LC substrate were employed as phase shifts. In [18], the feed phase of a patch array was tuned through an inverted microstrip line loaded with a 254 μm-thick LC substrate. Such phase-shifter structures are simple and intuitive but not easily integrable into systems. To change the resonant frequency of an antenna or its elements, some researchers have applied LC materials as the substrate of the working elements [18], [20]–[26]. Hu *et al.* [24] proposed an electronically tunable bandpass filter with a frequency-selective surface [24] consisting of a 130 μm-thick LC layer. In [26], a 510 μm-thick LC substrate enabled changeable resonant frequencies of a microstrip patch antenna. The LC-based reflectarray is an attractive option for microwave and millimeter-wave applications [14]. Several designs and investigations of LC-based reflectarrays can be found in the literature [12], [13], [23], [27]–[33]. Perez-Palomino *et al.* [12] achieved a wideband reflectarray at 100 GHz employing a multiresonant element with an 80 μm-thick LC. A phase-agile microstrip reflectarray with a 15 μm-thick LC layer enables operation at frequencies above 100 GHz [13]. A 35-GHz reconfigurable microstrip reflectarray utilized a highly anisotropic LC with a thickness of 127 μm [23]. Meanwhile, the modern LC filling process of an LC-display mass-production line limits the size of LC cells to several microns. In a more practical and low-cost LC-based reflectarray, the LC thickness should be less than 10 μm. A thinner LC layer is also expected to raise the switching speed. Therefore, developing an LC-based reflectarray with fast response speed remains a major challenge.

This article proposes a reconfigurable reflectarray with an 8 μm-thick LC. The reflectarray is designed, fabricated, and tested at 23.8 GHz. To realize a reconfigurable array, the 8 μm-thick LC material was designed as a varactor. The reflection phase of the proposed element is insensitive to the incident angle. A reconfigurable reflectarray composed of 26 × 38 identical LC-based elements was fabricated and tested. A microcontroller for driving the LC material was also designed and fabricated. The 32-channel microcontroller generates square-wave pulses with an ac voltage range from 0 to 11 V at 277 Hz. The proposed reconfigurable reflectarray antenna has a single-plane beam scanning capability from −60° to 60°.

Manuscript received July 7, 2021; revised October 10, 2021; accepted October 19, 2021. Date of publication November 10, 2021; date of current version April 7, 2022. This work was supported in part by the National Natural Science Foundation of China under Contract 61971254. *(Corresponding author: Zhijun Zhang.)*

The authors are with the Department of Electronic Engineering and the Beijing National Research Center for Information Science and Technology, Tsinghua University, Beijing 100084, China (e-mail: zjzh@tsinghua.edu.cn).

Color versions of one or more figures in this article are available at https://doi.org/10.1109/TAP.2021.3125378.

Digital Object Identifier 10.1109/TAP.2021.3125378

The 2-D scanning capability can be achieved by using a 1-D phased array as the feed.

The main contribution of this work is summarized as follows.

1) A new reconfigurable reflectarray with a thin (8 μm) LC layer is designed and fabricated. The thin LC layer improves the switching speed of the array. The proposed antenna is compatible with current LC display technology.
2) The LC material is deployed as a varactor rather than as a substrate for changing the reflection phase.
3) This work provides useful references for the design and measurement of reflectarray antennas based on continuously adjustable materials.

The remainder of this article is organized as follows. Section II presents and discusses the reflectarray element and its operating mechanism. Section III is devoted to the fabrication and performance measurements of the antenna. The work is summarized in Section IV.

II. Antenna Design

A. Reflectarray Element

The permittivity of LC can be altered by changing the applied quasi-static field. For this reason, LC material is frequently exploited in the design of reconfigurable reflectarray antennas [12], [13], [23], [27]–[32]. In most of the published works, the LC material is utilized as the substrate for changing the resonant frequency of the element. In [12] and [31], an LC-based substrate achieved tunable resonant frequency of a dipole element. Similarly, patch elements loaded with LC substrates have realized variable reflection phases [13], [28]–[30], [32]. The effects of LC anisotropy and inhomogeneity on the reflection phase have also been reported [34], [35]. Increasing the contributing volume of LC was found to enhance the effects of anisotropy and inhomogeneity. Usually, the impacts of anisotropy and inhomogeneity of LC cannot be ignored when loading LC as the substrate. This article proposes an element based on periodically loaded parallel H-shaped polygons with an 8 μm-thick LC and a small effectively biased region. In this design, different incident-wave angles and the LC inhomogeneity exert limited effects, as discussed next.

The proposed LC-based antenna cell is depicted in Fig. 1. The cell contains two substrates, three metal layers, and one LC layer. The LC material fills the cavity formed by the two substrates. A ground plane is loaded on the bottom layer of the lower substrate. An H-shaped polygon is periodically printed on the top and bottom surfaces of the lower and upper substrates, respectively [see Fig. 1(b)]. Two overlapping square areas exist between the adjacent H-shaped polygons in the +Z-direction (overlapping area II). The top and bottom copper layers are interconnected by the top and bottom bias lines, respectively. The two biased lines overlap in the +Z-direction (overlapping area I). For convenience, we refer to the LC regions between the two biasing lines and the LC regions between the overlapping square area (overlapping areas I and II, respectively) as LC-I and LC-II, respectively. LC-I and LC-II are collectively called LC-III. A quasi-static electric field is generated by the bias lines. The dielectric constant of LC-III can be tuned by changing the bias voltage. The varying permittivity of LC-I under different bias voltages negligibly affects the reflection phase of the reflectarray. This phenomenon will be explained later. The LC material is manufactured by BOE (Beijing, China), and its specification parameters (given by BOE) are $\varepsilon_{//} \approx 3.6$, $\varepsilon_{\perp} \approx 2.6$, and tan $\delta < 0.01$. The substrate is glass with a relative permittivity of $\varepsilon_r \approx 5.2$ and a loss tangent < 0.01. Table I gives the detailed dimensions of the reflectarray cell. In the present simulations, the maximum and minimum permittivities of LC were selected as 2.65 ($\varepsilon_{\perp}$) and 3.6 ($\varepsilon_{//}$), respectively.

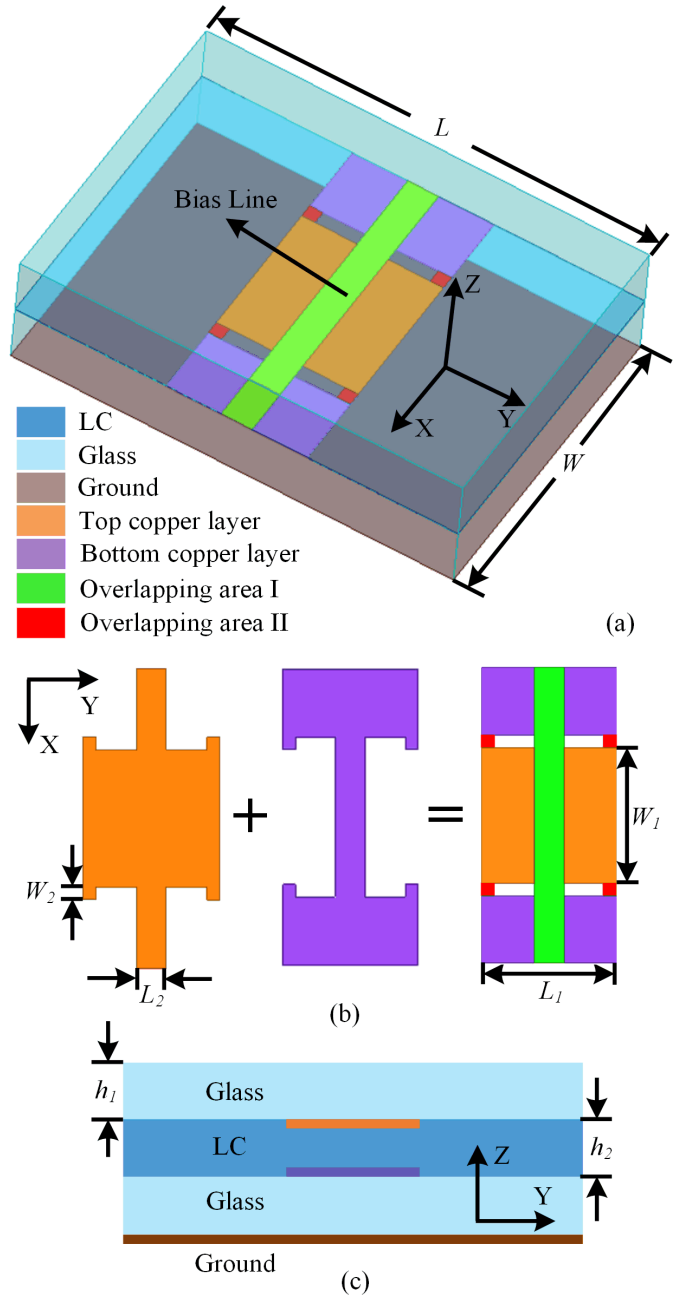

Fig. 1. Geometry of the reflectarray cell: (a) perspective view, (b) views of the top and bottom copper layers, and (c) side view.

TABLE I
DETAILED DIMENSIONS OF THE ANTENNA CELL

Parameter	Value(mm)	Parameter	Value(mm)
L	5	W_1	1.6
L_1	1.6	W_2	0.15
L_2	0.35	h_1	0.7
W	3.5	h_2	0.008

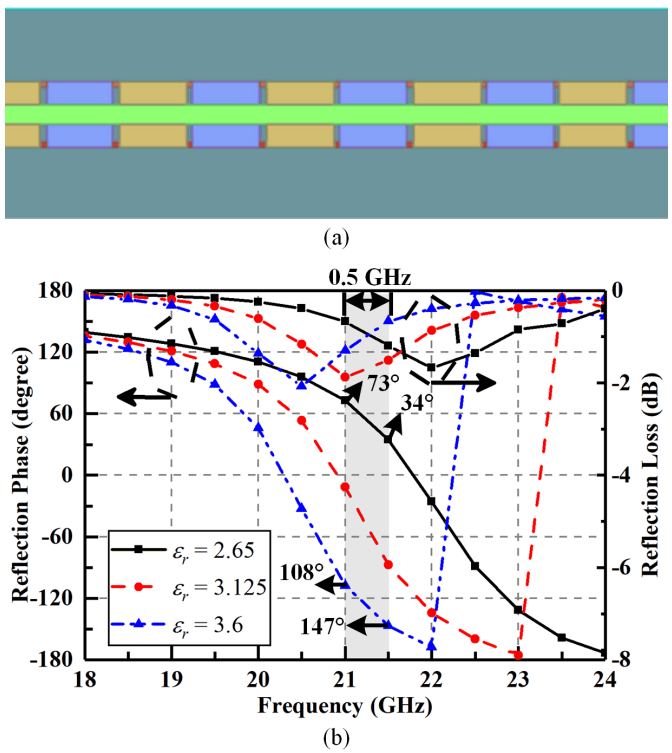

Fig. 2. (a) Basic row element of the proposed antenna. (b) Reflection phases and reflection losses as functions of frequency for different relative permittivities ε_r of LC-III.

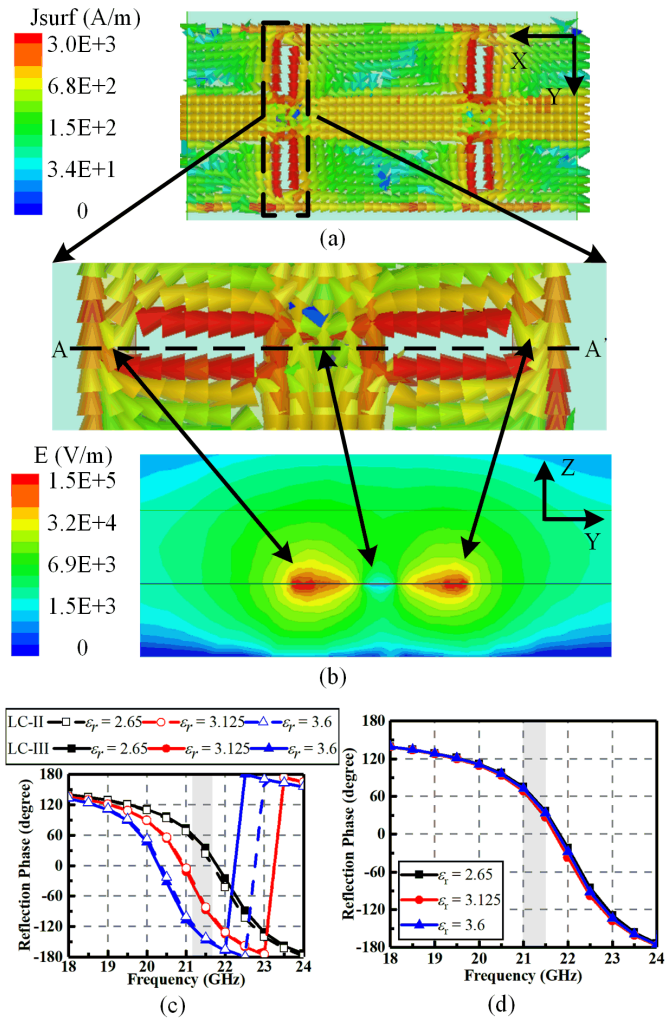

Fig. 3. (a) Simulated current distribution in the cell illuminated by normally incident X-polarized plane wave at 21 GHz. (b) Simulated E-field distribution on the *YZ* plane. Frequency responses of the reflection phases with different ε_r values of (c) LC-II and LC-III and (d) LC-I.

As the reflectarray is biased by rows [see Fig. 2(a)], the beams can steer only in one plane. The simulated reflection phases and reflection losses of the cell with periodic boundaries and different permittivities are depicted in Fig. 2(b). Changing the permittivity of LC-III from 2.65 to 3.6 induces a 180° phase shift with reflection losses of less than 2.5 dB in the 21.0–21.5 GHz range. The radiation performance can be improved by increasing the reflection-phase range [36]. In future work, the phase shift range can be enlarged by using multiresonant elements.

To reveal the operation principle of the reflectarray, the reflectarray cell was investigated in working mode. Fig. 3(a) plots the simulated current distribution in the cell under a normally incident X-polarized plane wave at 21 GHz. Part of the structure is enlarged to clarify the imagery. Half-wavelength loop modes were excited on both sides of the bias lines. Fig. 3(b) depicts the simulated E-field distribution on the *YZ* plane, where AA′ denotes the reference line. The electric field intensity is strong between the overlapping areas II and weak between overlapping areas I. Foreseeably, the LC-II works as a varactor that changed the resonant frequency of the loop mode. The altered LC-I's permittivity little affects the reflection phase. This concept was verified in two simulations. Fig. 3(c) plots the reflection phases as functions of the frequency with different ε_r values of the LC-II and LC-III regions. The simulated results with identical ε_r values of LC-II and LC-III agree well with each other, and changing the permittivity of LC-I negligibly affects the simulated reflection phase [see Fig. 3(d)]. Therefore, the influence of the permittivity of LC-I on the phase shift can be ignored.

Next, the sensitivity of the reflection phase to incident angle was investigated by varying the incident angle of illumination on the proposed cell. Fig. 4 compares the frequency responses of the reflection phase in LCs with different ε_r's at two incidence angles: $\theta = 0°$ and $\theta = 45°$. Here, θ is defined as the angle between $\boldsymbol{k}$ and the +Z-axis in the XZ plane. Relative to the reflection phases at $\theta = 0°$, the reflection phases at $\theta = 45°$ deviate by $-10°$, 6°, and 14° with

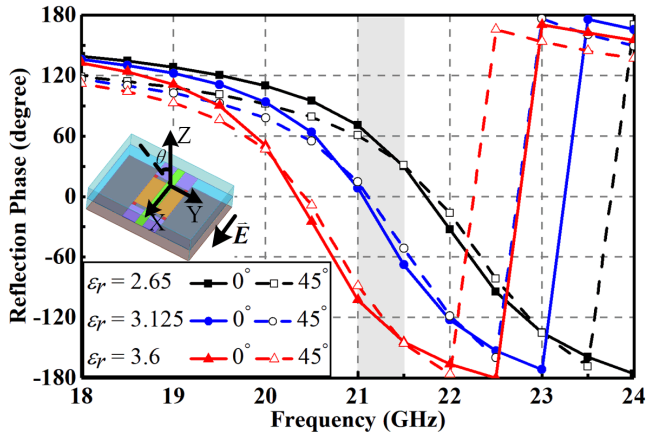

Fig. 4. Simulated frequency responses of the reflection phases of the LC-based cells with different relative permittivities, illuminated by an X-polarized plane wave at different incident angles θ.

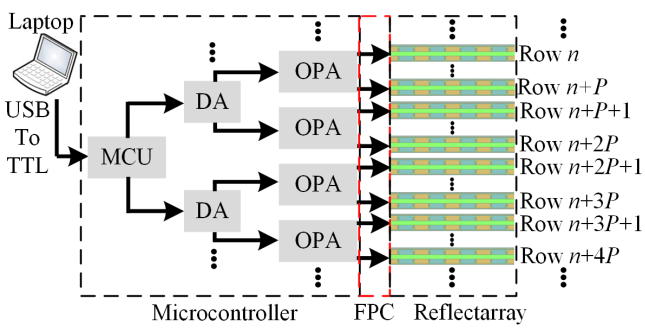

Fig. 5. Schematic of the control circuit.

$\varepsilon_r = 2.65$, 3.125, and 3.6, respectively, at 21 GHz. Similar results were obtained at 21.5 GHz, confirming the negligible effect of oblique incidence.

B. Control Circuit

Each element of an LC-based reflectarray can be biased by square pulses generated by a microcontroller. Fig. 5 shows a schematic of the control circuit. All bottom bias lines are gathered to provide the signal ground. Each of the top bias lines is connected from the glass to the flexible printed circuit (FPC). The microcontroller was designed to generate square waves with continuous ac voltage for biasing. The input is controlled by a microprogrammed control unit (MCU). The digital inputs from the MUC are transformed to analog signals by D–A converters. The appropriate voltage range can be obtained using operational amplifiers (OPAs). The MCU and laptop are linked by an USB to a transistor–transistor logic converter. Hence, the bias status of each element can be easily controlled by changing the input value on the PC.

C. Fabrication

Fig. 6(a) shows the manufactured reflectarray with 26 rows of basic elements. Each row contains 38 basic cells, as shown in Fig. 1(a). All the top bias lines are connected to the FPC.

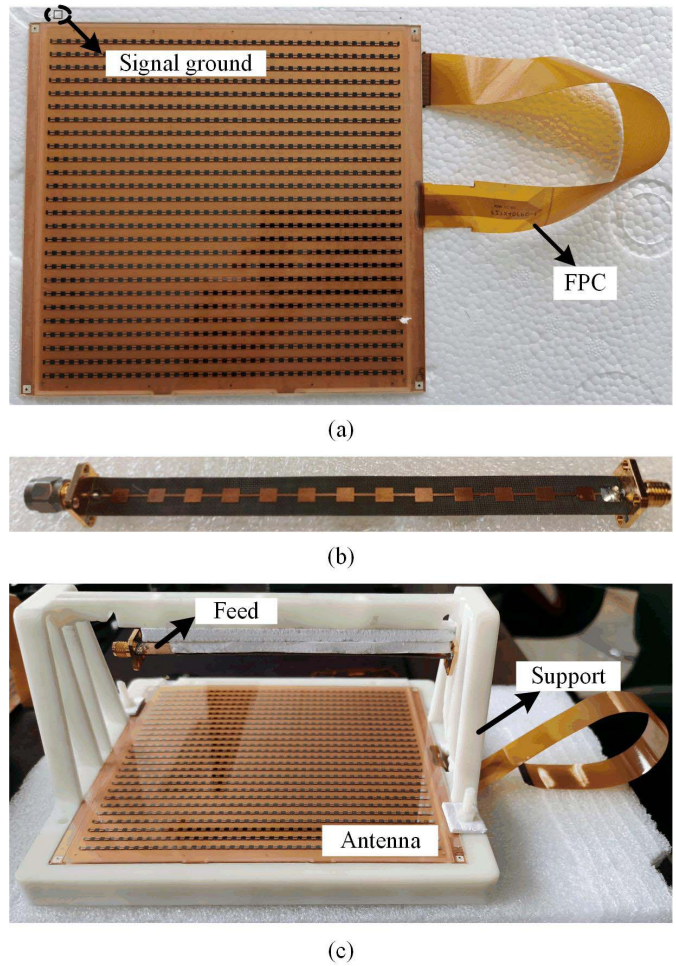

Fig. 6. (a) Photograph of the LC-based reflectarray. (b) Fabricated prototype of the series-fed microstrip antenna. (b) Fully assembled reflectarray with feed and support.

The fabrication technology is similar to normal LC display technology. In this work, the reflectarray was fed by a series-fed microstrip antenna, which was fabricated, as shown in Fig. 6(b). The reflectarray and feed antenna are fixed on plastic support fabricated using 3-D printing technology [see Fig. 6(c)]. The feed is placed directly above the reflectarray at a height of 49 mm. The feed is parallel to the element.

Fig. 7 shows the control circuit fabricated with printed circuit board technology. The control circuit includes one MCU (STM8L101g3u6), four DAs (R2A20168NP), and eight OPAs (ST LF347). The output of the control circuit was connected to the FPC of the reflectarray through an FPC connector (FH28-40S-0.5SH). A 277 Hz square wave with a bias voltage range of 0–11 V was generated by the control circuit.

III. Experimental Verification

A. Measurement Setup

Fig. 8 depicts the measurement setup of the experimental verification. The control circuit was driven by a direct voltage supplied by a dual dc power supply (LPS 202A). The bias voltage of each bias line was controlled by a laptop connected

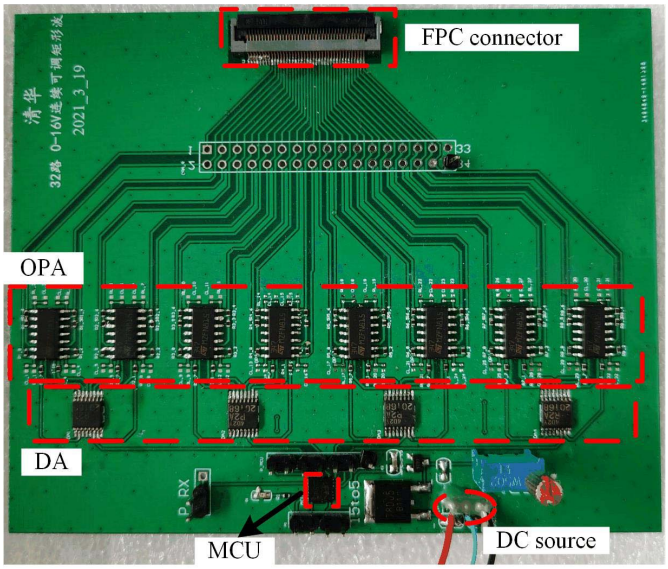

Fig. 7. Configuration of the microcontroller.

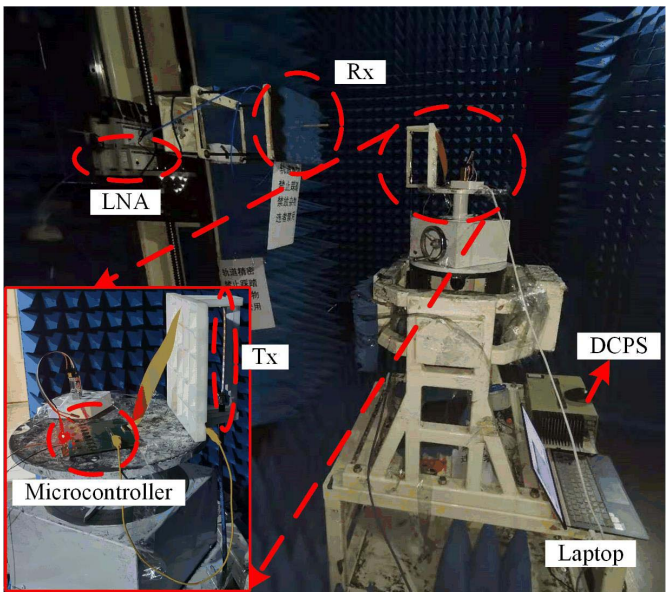

Fig. 8. Fully assembled measurement setup. DCPS: dual dc power supply; LNA: low-noise analyzer; Rx: receiver; and Tx: transmitter.

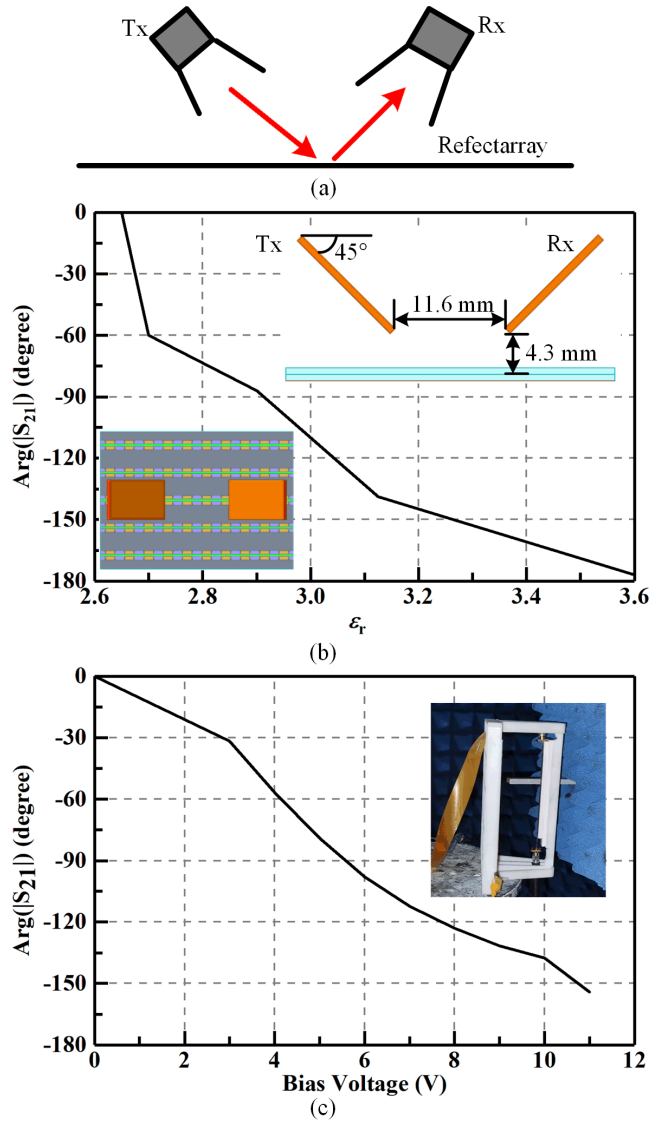

Fig. 9. (a) Schematic of the reflection phase test. Reflection phases of the reflectarray, (b) simulated for different ε_r values at 21.5 GHz, and (c) measured for different bias voltages at 23.8 GHz.

to the control circuit by a USB-to-TTL converter (HW-597). The fabricated series-fed microstrip antenna worked as a transmitter (Tx), while a rectangular waveguide worked as a receiver (Rx). The received signal was amplified by a low-noise amplifier (LNA). Measurements were performed in an anechoic chamber.

B. Reflection Phase Test

To measure the reflection phase of the fabricated reflectarray, the Rx was titled to receive the reflection wave, as shown in Fig. 9(a). Recall that the reflection phase of the proposed antenna is insensitive to the incident angle and is mainly determined by ε_r of the LC. The phase of $S_{Rx,Tx}$ is affected by the reflection from the partial area of the reflectarray. Predictably, the phase of $S_{Rx,Tx}$ can characterize (to some extent) the change in the reflection phase of the LC-based reflectarray with different ε_r's. This observation was demonstrated in a simulation. Two rectangular waveguides were used as the Tx and Rx [see Fig. 9(b)]. The simulated reflections for different ε_r's at 21.5 GHz were normalized, and the relative phase shift was approximately 180°. The simulated results demonstrate the effectiveness of the test method. When the same bias voltage (0–11 V) was applied to all rows during the measurement process, the phase of the receiving signal changed with different bias status. Fig. 9(c) depicts the tuning capability of the reflectarray at 23.8 GHz. The antenna generated an approximate relative phase shift of 150° at 23.8 GHz. The simulated operating frequency and the relative phase shift were 21.5 GHz and 180°, respectively. The

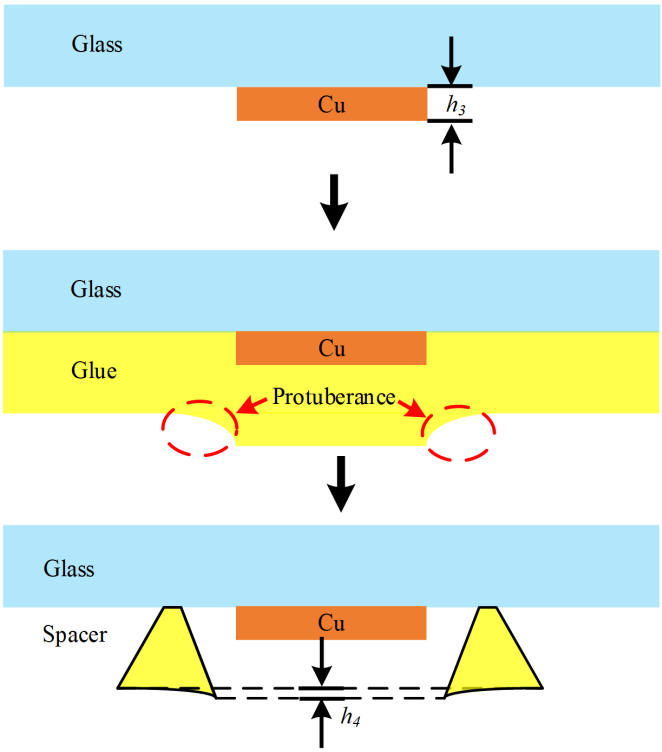

Fig. 10. Schematic of the fabricated process of the spacer.

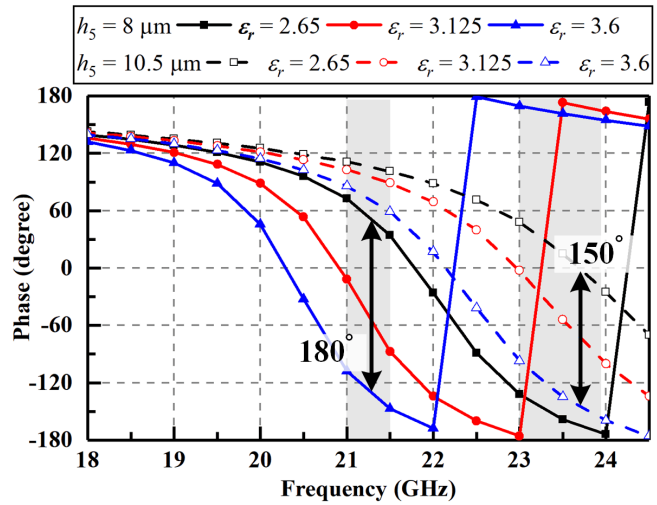

Fig. 11. Simulated reflection phases as functions of frequency in the LC-based cells with different LC heights h_5 between the top and bottom Cu layers, illuminated by X-polarized plane waves.

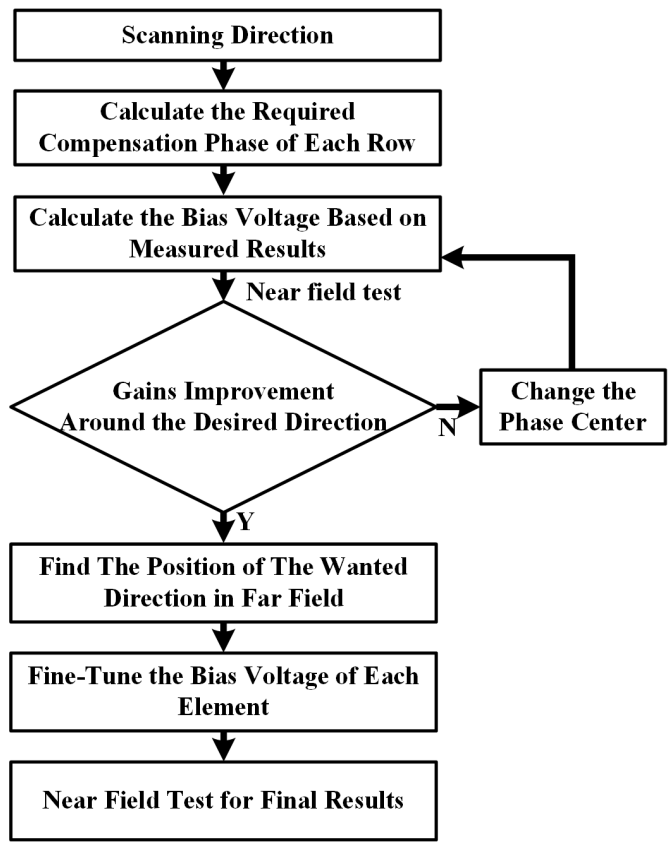

Fig. 12. Flowchart for the test process.

discrepancy between the simulated and measured results was mainly caused by fabrication errors.

The proposed antenna was fabricated similar to traditional LC displays, but the Cu deposition process differed and was rendered difficult by the relatively low working frequency in this study. A part of the fabrication process is shown in Fig. 10. Considering the skin effect in the microwave band, the Cu layer must be approximately 1.5 μm thick. As the Cu deposition process is not sufficiently mature to deposit 1 μm-thick coating, the real thickness of the Cu layer varied from 1.5 to 3.8 μm (h_3). A layer of glue was then attached to the surface. Because the Cu layer was thicker than 1 μm, the glue height was increased near the Cu. Spacers were obtained by eroding the unneeded parts of the glue. A height error h_4 caused by protuberance occurred in spacers near the Cu layer. The total fabrication error of the LC thickness (provided by BOE) was ~40%. Considering the nonnegligible fabrication error, the change of the operating frequency of the reflectarray was deemed reasonable. To demonstrate that the disagreement between the simulated and measured results was caused by the thickness error, we investigated the height of the LC layer (h_1). In the simulation, h_1 and h_3 were set to 13.5 and 1.5 μm, respectively (so the height of the LC layer between the top and bottom Cu layers was $h_5 = 10.5$ μm). Fig. 11 depicts the modified simulated results and the original simulated results.

The original simulated results ignore the height of the Cu layer with $h_5 = 8$ μm. The working frequency was higher, and the relative phase shift range was smaller in the modified case than that in the original case. The relative phase shift was approximately 150° near 23.5 GHz, consistent with the measured results.

C. Measurement of Radiation Patterns

Based on the measured relative phase shifts of the reflectarray, a test process was proposed, as shown in Fig. 12. First, the required compensation phase of each row element can be

TABLE II
APPLIED BIAS VOLTAGE CONFIGURATIONS

Beam direction	**Bias voltage (V)**												
0° (optimized)	0	7	11	0	4	11	11	0	3	5	8	11	11
0° (fine-tuned)	0	5	7	11	5.5	5	11	0	5	5	5	7	3
-40° (optimized)	11	0	0	0	0	3	3	4	3	3	0	0	0
-40° (fine-tuned)	0	4	0	3	6	4	4	2	11	5	4	4	1
-60° (optimized)	4	4	5	5	5	4	4	3	0	0	11	11	5
-60° (fine-tuned)	0	7	0	3	11	5	11	0	6	5	6	4	5
Row numbers	**1**	**2**	**3**	**4**	**5**	**6**	**7**	**8**	**9**	**10**	**11**	**12**	**13**
0° (optimized)	11	11	8	5	3	0	11	11	4	0	11	7	0
0° (fine-tuned)	3	7	5	5	5	0	11	5	5.5	11	8	5	0
-40° (optimized)	11	6	0	11	8	0	11	3	11	4	0	5	0
-40° (fine-tuned)	0	11	0	1	2	4	4	11	0	2	3	5	11
-60° (optimized)	0	11	6	0	11	0	11	0	11	0	7	0	4
-60° (fine-tuned)	3	7	7	7	3	6	5	5	5	9	0	2	5
Row numbers	**14**	**15**	**16**	**17**	**18**	**19**	**20**	**21**	**22**	**23**	**24**	**25**	**26**

TABLE III
COMPARISON AMONG THE PROPOSED LC-BASED REFLECTARRAY

Reference	[28]	[29]	[30]	[31]	[33]	Our work
Frequency (GHz)	77.2	75–79	77	96–102	35	23.7–24.2
Function of LC	Substrate	Substrate	Substrate	Substrate	Substrate	Varactor
Thickness of LC (um)	50	/	50	75	127	10.5
Scanning range (°)	25	12	20	60	20	60
Polarization	Linear	Linear	Linear	Linear	Linear	Linear
Aperture efficiency (%)	/	/	/	1.8	9.2	5.8
Max gain (dB)	/	25.1	/	19.4	19.5	18.9

obtained from the reflectarray parameters, the height of the feed, and the considered scanning direction. Second, the bias voltage of each element is calculated based on the measured relative phase shift. The bias voltage can be varied by selecting different phase centers of the measured results. Third, the radiation patterns are measured in an antenna near-field test. If the measured gains around the desired direction are not improved, the phase center should be reselected. The fourth step finds the position of the desired radiation direction in the far-field. Fifth, the bias voltage of each row is fine-tuned to improve the gain (measured S_{21}) in the desired direction. The final measured patterns are then obtained in a near-field test.

Applying the above process, far-field measurements at 23.8 GHz were obtained in an anechoic chamber. Fig. 13 plots the measured results of the realized reflectarray for three main-beam directions: 0°, −40°, and −60°. The results were optimized using the calculated bias voltages. The final results (fine-tuned results) were obtained by fine-tuning the calculated bias voltage of each bias line. The corresponding bias voltages of the optimized and fine-tuned results are listed in Table II. The discrepancy in the bias voltages of the optimized and fine-tuned results was mainly caused by fabrication error. As shown in Fig. 13, the gain in the desired direction was higher in the fine-tuned results than in the optimized results, thereby validating the test process. The measured gain of the feed at 23.8 GHz was 15.5 dB. The final measured gains of the antenna oriented at 0°, −40°, and −60° were 18.1, 18.4, and 18.9 dB, respectively. The broadside gain was limited by the blocking effect of the feed and support. The high sidelobe level presented in Fig. 13(b) and (c) was mainly caused by phase quantization error [36]. The steering ability of the proposed reflectarray is not limited to the abovementioned directions. In fact, the main beam can be continuously steered to wide angles by virtue of the continuously adjustable capabilities of LC. In summary, the main lobes were successfully steered to the desired directions through the optimization routine.

Table III summarizes the electrical performances of this work and other LC-based reflectarray antennas. The proposed antenna has a thinner LC layer and a wider scanning range than the other antennas. The LC material was employed as a varactor in this work; in the previous studies, it was employed as the substrate for tuning the reflection phase.

IV. CONCLUSION

This article investigated a reconfigurable LC-based reflectarray. The antenna element is constructed by periodically loading H-shaped polygons. An 8 μm-thick LC layer is loaded as a varactor. In the simulation study, the basic element achieved a relative phase shift of 180°. A reflectarray with 26 rows of the basic element was then fabricated and tested. The refractarray was illuminated under a series-fed microstrip antenna, and a 32-channel control circuit was designed for biasing. The

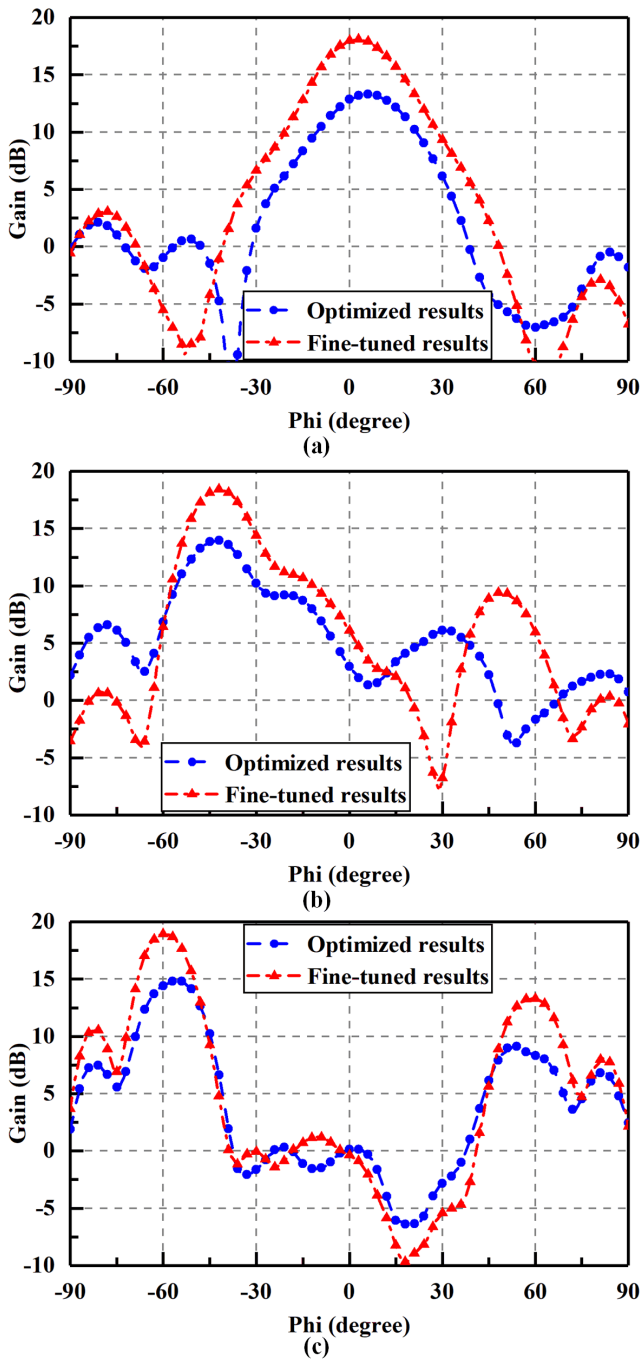

Fig. 13. Measured far-field patterns at 23.8 GHz for different main-beam directions: (a) 0°, (b) −40°, and (c) −60°.

disagreements between the measured and simulated results were studied and discussed. The antenna patterns in the desired main-beam directions were measured at 23.8 GHz through the proposed test process. The beam steering capability in one plane of the reflectarray was validated at different steering directions of the main beam (0°, −40°, and −60°). Scanning in another plane can be achieved by designing a 1-D phase array as the feed. The proposed design scheme offers a new solution to the design and measurement of LC-based reflectarray antennas.

Acknowledgment

The authors thank BOE for manufacturing the liquid crystal (LC) panels and providing technical support. They are also grateful to Mr. T. Ting and Mrs. C. Tang of BOE for fruitful discussions.

References

[1] J. Huang and J. A. Encinar, *Reflectarray Antennas*. Hoboken, NJ, USA: Wiley, 2007.

[2] M. Riel and J.-J. Laurin, "Design of an electronically beam scanning reflectarray using aperture-coupled elements," *IEEE Trans. Antennas Propag.*, vol. 55, no. 5, pp. 1260–1266, May 2007.

[3] S. V. Hum, M. Okoniewski, and R. J. Davies, "Realizing an electronically tunable reflectarray using varactor diode-tuned elements," *IEEE Microw. Wireless Compon. Lett.*, vol. 15, no. 6, pp. 422–424, Jun. 2005.

[4] E. Carrasco, M. Barba, and J. A. Encinar, "X-band reflectarray antenna with switching-beam using PIN diodes and gathered elements," *IEEE Trans. Antennas Propag.*, vol. 60, no. 12, pp. 5700–5708, Dec. 2012.

[5] H. Kamoda, T. Iwasaki, J. Tsumochi, and T. Kuki, "60-GHz electrically reconfigurable reflectarray using p-i-n diode," in *IEEE MTT-S Int. Microw. Symp. Dig.*, Boston, MA, USA, Jun. 2009, pp. 1177–1180.

[6] L. Rajagopalan, Y. Rahmat-Samii, and W. A. Imbriale, "RF MEMS actuated reconfigurable reflectarray patch-slot element," *IEEE Trans. Antennas Propag.*, vol. 56, no. 12, pp. 3689–3699, Dec. 2008.

[7] O. Bayraktar, O. A. Civi, and T. Akin, "Beam switching reflectarray monolithically integrated with RF MEMS switches," *IEEE Trans. Antennas Propag.*, vol. 60, no. 2, pp. 854–862, Feb. 2012.

[8] J. Perruisseau-Carrier and A. Skrivervik, "Monolithic MEMS-based reflectarray cell digitally reconfigurable over a 360° phase range," *IEEE Antennas Wireless Propag. Lett.*, vol. 7, pp. 138–141, 2008.

[9] K. K. Karnati, Y. Shen, M. E. Trampler, S. Ebadi, P. F. Wahid, and X. Gong, "A BST-integrated capacitively loaded patch for K_a and X-band beamsteerable reflectarray antennas in satellite communications," *IEEE Trans. Antennas Propag.*, vol. 63, no. 4, pp. 1324–1333, Jan. 2015.

[10] V. G. Kononov, C. A. Balanis, A. C. Polycarpou, and C. R. Birtcher, "Non-uniform field modeling of ferrite-loaded cavity-backed slot antennas," *IEEE Trans. Antennas Propag.*, vol. 57, no. 10, pp. 3402–3405, Oct. 2009.

[11] L. Cai, Z. H. Jiang, and W. Hong, "Evaluation of reconfigurable reflectarray antenna element at 19 GHz based on highly anisotropic liquid crystal material," in *Proc. IEEE Int. Conf. Comput. Electromagn. (ICCEM)*, Mar. 2019, pp. 1–3, doi: 10.1109/COMPEM.2019.8778849.

[12] G. Perez-Palomino *et al.*, "Design and experimental validation of liquid crystal-based reconfigurable reflectarray elements with improved bandwidth in F-band," *IEEE Trans. Antennas Propag.*, vol. 61, no. 4, pp. 1704–1713, Apr. 2013.

[13] W. Hu *et al.*, "Design and measurement of reconfigurable millimeter wave reflectarray cells with nematic liquid crystal," *IEEE Trans. Antennas Propag.*, vol. 56, no. 10, pp. 3112–3117, Oct. 2008.

[14] T. L. Ting, "Technology of liquid crystal based antenna," *Opt. Exp.*, vol. 27, no. 12, pp. 17138–17153, 2019.

[15] R. Hosono, Y. Uemichi, Y. Hasegawa, Y. Nakatani, K. Kobayashi, and N. Guan, "Development of millimeter wave devices based on liquid crystal polymer (LCP) substrate," *IEICE Electro. Exp.*, vol. 14, no. 20, pp. 1–13, 2017.

[16] O. H. Karabey, S. Bildik, S. Bausch, S. Strunck, A. Gaebler, and R. Jakoby, "Continuously polarization agile antenna by using liquid crystal-based tunable variable delay lines," *IEEE Trans. Antennas Propag.*, vol. 61, no. 1, pp. 70–76, Jan. 2013.

[17] J. Shu, H. Peng, Y. Zhang, and J. Mao, "A dual polarized pattern reconfigurable antenna array using liquid crystal phase shifter," in *Proc. Int. Symp. Antennas Propag. (ISAP)*, 2018, pp. 1–2.

[18] Y. Zhao, C. Huang, A. Qing, and X. Luo, "A frequency and pattern reconfigurable antenna array based on liquid crystal technology," *IEEE Photon. J.*, vol. 9, no. 3, Jun. 2017, Art. no. 4600307.

[19] M. Nestoros, N. C. Papanicolaou, and A. C. Polycarpou, "Design of beam-steerable array for 5G applications using tunable liquid-crystal phase shifters," in *Proc. 13rd Eur. Conf. Antennas Propag. (EuCAP)*, 2019, pp. 1–4.

[20] G. S. Sethi, A. Srivastava, C.-Y. Chiu, V. Chigrinov, and R. D. Murch, "Design of a transparent LC based reconfigurable antenna," in *Proc. Asia–Pacific Microw. Conf. (APMC)*, New Delhi, India, Dec. 2016, pp. 1–5.

[21] Y. Lan, T. Zhang, and D. Jiang, "K-band liquid-crystal-based frequency and pattern reconfigurable linear antenna array," in *IEEE MTT-S Int. Microw. Symp. Dig.*, Chengdu, China, May 2018, pp. 1–6.

[22] Z. Wang, Y. Liu, and D. Jiang, "K-band liquid-crystal-based frequency reconfigurable conformal array antenna," in *Proc. Int. Conf. Microw. Millim. Wave Technol. (ICMMT)*, May 2019, pp. 1–4, doi: 10.1109/ICMMT45702.2019.8992061.

[23] R. Marin, A. Mossinger, J. Freese, A. Manabe, and R. Jakoby, "Realization of 35 GHz steerable reflectarray using highly anisotropic liquid crystal," in *Proc. IEEE Antennas Propag. SoC. Int. Symp.*, Dec. 2006, pp. 4307–4310.

[24] W. Hu *et al.*, "Liquid crystal tunable mm wave frequency selective surface," *IEEE Microw. Wireless Compon. Lett.*, vol. 17, no. 9, pp. 667–669, Sep. 2007.

[25] J. Kim and J. Oh, "Liquid-crystal-embedded aperture-coupled microstrip antenna for 5G applications," *IEEE Antennas Wireless Propag. Lett.*, vol. 19, no. 11, pp. 1958–1962, Nov. 2020.

[26] A. C. Polycarpou, M. A. Christou, and N. C. Papanicolaou, "Tunable patch antenna printed on a biased nematic liquid crystal cell," *IEEE Trans. Antennas Propag.*, vol. 62, no. 10, pp. 1980–1987, Oct. 2014.

[27] C.-H. Zhao, Q. Wu, and F.-Y. Meng, "Design of reconfigurable circularly polarized reflectarray antenna at 100 GHz based on liquid crystals," in *Proc. Int. Conf. Microw. Millimeter Wave Technol. (ICMMT)*, May 2019, pp. 1–4.

[28] A. Gaebler *et al.*, "Liquid crystal-reconfigurable antenna concepts for space applications at microwave and millimeter waves," *Int. J. Antennas Propag.*, vol. 2009, Feb. 2009, Art. no. 876989, doi: 10.1155/2009/876989.

[29] S. Bildik, S. Dieter, C. Fritzsch, W. Menzel, and R. Jakoby, "Reconfigurable folded reflectarray antenna based upon liquid crystal technology," *IEEE Trans. Antennas Propag.*, vol. 63, no. 1, pp. 122–132, Jan. 2015.

[30] S. Bildik *et al.*, "Reconfigurable liquid crystal reflectarray with extended tunable phase range," in *Proc. 8th Eur. Radar Conf. (EuRAD)*, Manchester, U.K., Oct. 2011, pp. 404–407.

[31] G. Perez-Palomino *et al.*, "Design and demonstration of an electronically scanned reflectarray antenna at 100 GHz using multiresonant cells based on liquid crystals," *IEEE Trans. Antennas Propag.*, vol. 63, no. 8, pp. 3722–3727, Aug. 2015.

[32] J. Yang *et al.*, "Reflective liquid crystal terahertz phase shifter with tuning range of over 360°," *IET Microw., Antennas Propag.*, vol. 12, no. 9, pp. 1466–1469, Jul. 2018.

[33] A. Moessinger *et al.*, "Electronically reconfigurable reflectarray with nematic liquid crystal," *Electron. Lett.*, vol. 42, no. 16, pp. 899–900, Aug. 2006.

[34] G. Perez-Palomino *et al.*, "Accurate and efficient modeling to calculate the voltage dependence of liquid crystal-based reflectarray cells," *IEEE Trans. Antennas Propag.*, vol. 62, no. 5, pp. 2659–2668, May 2014.

[35] G. Perez-Palomino, J. A. Encinar, and M. Barba, "Accurate electromagnetic modeling of liquid crystal cells for reconfigurable reflectarrays," in *Proc. 5th Eur. Conf. Antennas Propag. (EUCAP)*, Apr. 2011, pp. 997–1001.

[36] H. Yang *et al.*, "A study of phase quantization effects for reconfigurable reflectarray antennas," *IEEE Antennas Wireless Propag. Lett.*, vol. 16, pp. 302–305, 2016.

Weiquan Zhang received the B.S. degree from the University of Electronic Science and Technology of China, Chengdu, China, in 2018. He is currently pursuing the Ph.D. degree in electrical engineering with Tsinghua University, Beijing, China.

His current research interests include reconfigurable antennas, multimode antennas, and reflectarray antennas.

Yue Li (Senior Member, IEEE) received the B.S. degree in telecommunication engineering from Zhejiang University, Zhejiang, China, in 2007, and the Ph.D. degree in electronic engineering from Tsinghua University, Beijing, China, in 2012.

In June 2012, he was a Post-Doctoral Fellow with the Department of Electronic Engineering, Tsinghua University. In December 2013, he was a Research Scholar with the Department of Electrical and Systems Engineering, University of Pennsylvania, Philadelphia, PA, USA. He was a Visiting Scholar with Institute for Infocomm Research (I2R), Agency for Science, Technology and Research (A*STAR), Singapore, in 2010, and the Hawaii Center of Advanced Communication (HCAC), University of Hawaii at Manoa, Honolulu, HI, USA, in 2012. Since January 2016, he has been with Tsinghua University, where he is currently an Assistant Professor. He is also an Associate Professor with the Department of Electronic Engineering, Tsinghua University. He has authored or coauthored over 160 journal articles and 50 international conference papers. He holds 20 granted Chinese patents. His current research interests include metamaterials, plasmonics, electromagnetics, nanocircuits, mobile and handset antennas, MIMO and diversity antennas, and millimeter-wave antennas and arrays.

Dr. Li was a recipient of the Issac Koga Gold Medal from the URSI General Assembly in 2017; the Second Prize of Science and Technology Award of the China Institute of Communications in 2017; the Young Scientist Awards from the conferences of Progress in Electromagnetics Research Symposium (PIERS) in 2019, International Applied Computational Electromagnetics Society Symposium (ACES) in 2018, Atlantic Radio Science Conference (AT-RASC) in 2018, Asia–Pacific Radio Science Conference (AP-RASC) in 2016, International Symposium on Electromagnetic Theory (EMTS) in 2016, and General Assembly of the International Union of Radio Science (URSI GASS) in 2014; the Best Paper Awards from the conferences of International Symposium on Antennas and Propagation (ISAP) in 2019, Cross Strait Quad-Regional Radio Science and Wireless Technology Conference (CSQRWC) in 2018, National Conference on Microwave and Millimeter Wave in China (NCMMW) in 2017 and 2018, Asia–Pacific Conference on Antennas and Propagation (APCAP) in 2017, National Conference on Antennas (NCANT) in 2017 and 2019, International Symposium on Antennas, Propagation and EM Theory (ISAPE) in 2016, and International Conference on Microwave and Millimeter Wave Technology (ICMMT) in 2016; the Outstanding Doctoral Dissertation of Beijing Municipality in 2013; and the Principal Scholarship of Tsinghua University in 2011. He is also serving as an Associate Editor for IEEE TRANSACTIONS ON ANTENNAS AND PROPAGATION, IEEE ANTENNAS AND WIRELESS PROPAGATION LETTERS, *Microwave and Optical Technology Letters*, *Computer Applications in Engineering Education*, and the Editorial Board of *Scientific Reports*.

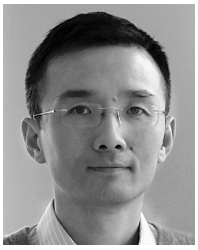

Zhijun Zhang (Fellow, IEEE) received the B.S. and M.S. degrees from the University of Electronic Science and Technology of China, Chengdu, China, in 1992 and 1995, respectively, and the Ph.D. degree from Tsinghua University, Beijing, China, in 1999.

In 1999, he was a Post-Doctoral Fellow with the Department of Electrical Engineering, The University of Utah, Salt Lake City, UT, USA, where he was appointed as a Research Assistant Professor in 2001. In May 2002, he was an Assistant Researcher with the University of Hawaii at Manoa, Honolulu, HI, USA. In November 2002, he joined Amphenol T&M Antennas, Vernon Hills, IL, USA, as a Senior Staff Antenna Development Engineer, and was then promoted to the position of Antenna Engineer Manager. In 2004, he joined Nokia Inc., San Diego, CA, USA, as a Senior Antenna Design Engineer. In 2006, he joined Apple Inc., Cupertino, CA, USA, as a Senior Antenna Design Engineer, and was then promoted to the position of Principal Antenna Engineer. Since August 2007, he has been with Tsinghua University, where he is currently a Professor with the Department of Electronic Engineering. He is the author of *Antenna Design for Mobile Devices* (Wiley, first edition, 2011, and second edition, 2017).

Dr. Zhang has served as an Associate Editor for the IEEE TRANSACTIONS ON ANTENNAS AND PROPAGATION from 2010 to 2014 and the IEEE ANTENNAS AND WIRELESS PROPAGATION LETTERS from 2009 to 2015.